BJR https://doi.org/10.1259/bjr.20230298

Received: 30 March 2023 | Accepted: 30 July 2023 | Published online: 09 October 2023

Cite this article as:
Chaudhari AJ, Lim Y, Cui SX, Bayne CO, Szabo RM, Boutin RD, et al. Real-time MRI of the moving wrist at 0.55 tesla. *Br J Radiol* (2023) 10.1259/bjr.20230298.

SHORT COMMUNICATION

Real-time MRI of the moving wrist at 0.55 tesla

[1]ABHIJIT J CHAUDHARI, PhD, [2]YONGWAN LIM, PhD, [3]SOPHIA X. CUI, PhD, [4]CHRISTOPHER O. BAYNE, MD, [4]ROBERT M. SZABO, MD, MPH, [5]ROBERT D. BOUTIN, MD and [2]KRISHNA S NAYAK, PhD

[1]Department of Radiology, University of California, Davis, Sacramento, CA, USA
[2]Ming Hsieh Department of Electrical and Computer Engineering, University of Southern California, Los Angeles, CA, USA
[3]Siemens Medical Solutions USA Inc., Malvern, PA, USA
[4]Department of Orthopaedic Surgery, University of California Davis, Sacramento, CA, USA
[5]Department of Radiology, Stanford University School of Medicine, Stanford, CA, USA

Address correspondence to:
Dr Abhijit J Chaudhari
E-mail: *ajchaudhari@ucdavis.edu*
Dr Krishna S Nayak
E-mail: *knayak@usc.edu*

Objectives: Magnetic resonance imaging (MRI) using 1.5T or 3.0T systems is routinely employed for assessing wrist pathology; however, due to off-resonance artifacts and high power deposition, these high-field systems have drawbacks for real-time (RT) imaging of the moving wrist. Recently, high-performance 0.55T MRI systems have become available. In this proof-of-concept study, we tested the hypothesis that RT-MRI during continuous, active, and uninterrupted wrist motion is feasible with a high-performance 0.55T system at temporal resolutions below 100 ms and that the resulting images provide visualization of tissues commonly interrogated for assessing dynamic wrist instability.

Methods: Participants were scanned during uninterrupted wrist radial-ulnar deviation and clenched fist maneuvers. Resulting images (nominal temporal resolution of 12.7–164.6 ms per image) were assessed for image quality. Feasibility of static MRI to supplement RT-MRI acquisition was also tested.

Results: The RT images with temporal resolutions < 100 ms demonstrated low distortion and image artifacts, and higher reader assessment scores. Static MRI scans showed the ability to assess anatomical structures of interest in the wrist.

Conclusion: RT-MRI of the wrist at a high temporal resolution, coupled with static MRI, is feasible with a high-performance 0.55T system, and may enable improved assessment of wrist dynamic dysfunction and instability.

Advances in knowledge: Real-time MRI of the moving wrist is feasible with high-performance 0.55T and may improve the evaluation of dynamic dysfunction of the wrist.

INTRODUCTION

Wrist motion is facilitated by a complex interplay between carpal bones and carpal ligaments, with the latter constraining range of motion and providing stability.[1] A detailed understanding of the functional kinematics of wrist tissues necessary to carry out activities of daily living[2] is essential to effectively diagnose and treat wrist dysfunction. To facilitate such an understanding, there is a need for techniques that enable the direct visualization of wrist tissues during active motion or loading.[3]

Magnetic Resonance Imaging (MRI) is commonly employed to evaluate wrist pathology. Standard MRI acquisition, however, is slow and precludes the capture of wrist motion and dynamic pathologies of interest in assessing dynamic instability.[4] To address this shortcoming, real-time MRI (RT-MRI) protocols, typically using 1.5T and 3T MRI scanners, have been developed.[5–7] These protocols, however, have suffered from a relatively slow image acquisition rate that is inadequate for tracking wrist motion at natural speeds, and image artifacts that frequently obscure critical wrist structures.

The trend in modern MRI systems has been to reach for higher field strengths (*e.g.,* 3T, 7T), which has served static wrist imaging well. However, these field strengths correspond to increased distortion and signal loss for RT-MRI of the moving joints, such as those of the wrist.[4,6] Recently, high-performance 0.55T MRI scanners have shown unique characteristics that are beneficial for wrist RT imaging.[8] In particular, the high-performance 0.55T systems offer a high acquisition duty cycle, typically achieved using efficient k-space trajectories, not possible or practical at higher field strengths and resulting in the mitigation of image

artifacts.[9] These systems can further utilize pulse sequences, such as balanced steady-state press precession (bSSFP), that provide superior signal-to-noise ratio and efficiency enabling a vast increase in imaging speed compared to higher field system.[10] The feasibility of high-performance 0.55T for dynamic wrist imaging has not been evaluated to date and is the purpose of this work.

We conducted a first-in-human study utilizing a high-performance 0.55T system and RT-MRI acquisition to assess tissues of the actively moving wrist during uninterrupted radial-ulnar deviation (RUD) and clenched fist maneuvers. These maneuvers were chosen because of their significance in evaluating dynamic carpal instability.[11] We assessed the impact of increasing the temporal resolution on imaging metrics pertaining to the assessment of the wrist's functional kinematics. Further, we tested the feasibility of a static wrist MRI protocol at high-performance 0.55T to supplement the RT-MRI acquisition.

METHODS

Study participants

This prospective study received institutional review board approval and informed consent was obtained from all particicpants. The study cohort consisted of five participants, three men and two women, with age [median (range)] of 46 (31–59) years. No prospective sample size calculation was performed given the pilot nature of the study. Three participants underwent RT-MRI and static MRI, while two participants underwent only static MRI. Inclusion criteria were healthy, asymptomatic subjects between the ages of 18–70 years without a history of wrist trauma, wrist pain, or prior wrist surgery. Subjects were excluded if they had a contraindication to MRI or could not complete the wrist MRI examination.

MRI protocol

Participants underwent wrist scanning on a whole body 0.55T MRI system (prototype MAGNETOM Aera XQ, Siemens Healthineers, Erlangen, Germany) equipped with contemporary high-performance hardware and software capabilities (hence termed high-performance 0.55T[8]). The system is equipped with high-performance shielded Aera XQ gradients (Siemens Healthineers, Erlangen, Germany), providing 45 mT/m amplitude, and 200 T/m/s slew rate.[8] The right wrist was scanned. The participants lay prone on the scanner bed with one arm placed on the integrated spine RF coil (below) and a 6-channel surface body coil (above), in a configuration that did not restrict wrist range of motion (Figure 1). For RT-MRI acquisition, a coronal slice showing the scapholunate (SL) interval was prescribed based on the localizer scan. Each participant performed two wrist maneuvers (RUD and the clenched fist maneuver) during RT-MRI acquisition utilizing their full, active range-of-motion at their natural speed (*i.e.*, completing at least two cycles of each maneuver in under 5 s). The RT-MRI acquisition consisted of a 2D spiral balanced-steady-state-free-precession (bSSFP) pulse sequence (in-plane resolution: =1.38×1.38 mm^2, slice thickness = 6 or 8 mm). Data were reconstructed with nominal temporal resolutions of 164.6 ms (full sampling), and 12.7, 25.3, 38.0, 63.3, and 101.3 ms per slice, representing undersampling by factors of 92%, 85%, 77%, 62 and 38%, respectively. Other details of the image acquisition and reconstruction are provided in the Supplemental Section S.1.

For static imaging of the immobilized wrist in the neutral position, the acquisition involved a T_1-weighted (T_1w) gradient-recalled-echo-based 3D pulse sequence with voxel size of 0.61 × 0.61×0.60 mm^3, and 2D proton-density weighted (PDw, coronal) and T_1w (coronal and axial) turbo spin echo (TSE) acquisitions with in-plane resolutions of 0.31 × 0.31 and 0.25 × 0.25 mm^2, and slice thicknesses of 2.5 and 3.0 mm, respectively. Detailed sequence parameters are summarized in Supplemental Section S.2. Static MR images were reconstructed using the standard method provided by the system manufacturer.

Figure 1. Photographs showing the positioning of a study participant on the scanner bed of the high-performance 0.55T system.

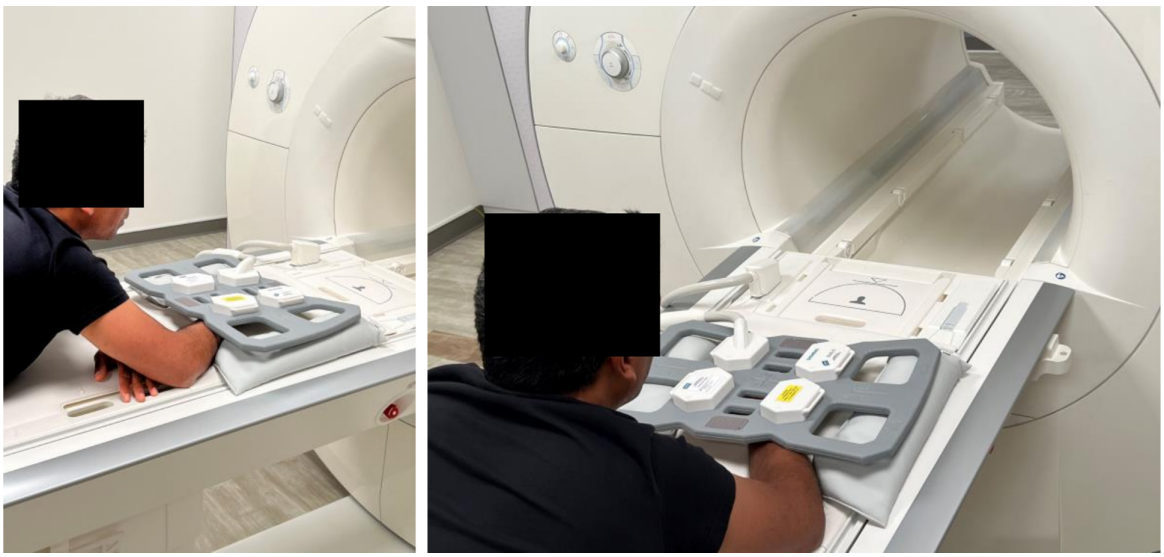

Table 1. Reader scoring of overall image quality

Score	Description
1	Extremely poor, defined as 'major artifacts exist, and the images are not analyzable.'
2	Poor, defined as 'major artifacts exist, and use is, therefore, analysis is not advised'
3	Average, defined as 'borderline analyzable due to the image quality'
4	Good, defined as 'containing minor artifacts which do not adversely affect analysis'
5	Excellent, defined as 'no artifacts'

Image reconstruction and analysis

The RT-MR images underwent two types of evaluation by independent experienced readers, the first evaluating overall image quality and the second assessing specific imaging features. First, two readers, a fellowship-trained musculoskeletal radiologist with 24 years of post-training experience, and a PhD scientist with expertise in musculoskeletal and wrist imaging for 15 years, scored the images (scoring scale is in Table 1). Second, two imaging features, the SL interval and the capitate-triquetral (CT) interval, were evaluated from the images (scoring scale is in Table 2).

The static MRI scans were also assessed based on the scales in Tables 1 and 2. Further, visualization of the sharpness of joint borders, contrast between intraarticular fluid and surrounding structures, and the ability to assess the triangular fibrocartilage complex (TFCC) was evaluated. Each of these factors was graded poor, fair, or good.

Statistical analysis

The median and interquartile range of the pooled reader scores were calculated. These values were compared across temporal resolutions and slice thickness using the Mann-Whitney U-test in the R Statistical Software (v4.1.0; 2021). Results were considered significant at $p < 0.05$. Intraclass correlation coefficient (ICC) estimates were also calculated in R, based on a mean-rating, absolute-agreement, two-way mixed-effects model. Reader scores, unless otherwise specified, are provided as median (interquartile range).

RESULTS

Imaging of the wrist at high-performance 0.55T

Representative static MR images of the wrist are shown in Figure 2. Representative high-performance 0.55T images of the wrist during the active RUD maneuver at different nominal temporal resolutions are shown in Figure 3. Representative images at different reader score levels are shown in Supplemental Figure 1. Videos are provided as Supplemental Videos 1–3. There was good inter-rater reliability (ICC = 0.77).

Table 2. Reader scoring of the SL and CT interval

Score	Description
1	Not visualized
2	Visualized but not well-defined
3	Well defined

Temporal resolutions under 100 ms provided improved reader assessment scores than those greater than 100 ms for RUD but not for the clenched fist maneuver

The evaluated images had temporal resolutions ranging from 12.7 ms (79.4 frames per sec, highest temporal resolution) to 164.6 ms (6.1 frames per sec, lowest temporal resolution), the latter involving full k-space sampling. The overall reader assessment scores for images collected during the RUD maneuver were unchanged for scans with temporal resolutions of <100 ms and were higher than those with temporal resolutions of >100 ms ($p < 0.05$) (Table 3). For temporal resolutions < 100 ms, images of all study participants for the RUD maneuver had a median overall score of ≥3 (Table 3). While not directly impacting scores, the readers noted that despite minor artifacts such as streaking, images at increased temporal resolutions show reduced motion blurring and a sharper boundary between the scaphoid and lunate or between the capitate and triquetrum (Figure 3). This impact was pronounced for scans performed during RUD compared to the clenched fist maneuver, given the larger overall tissue displacement in the former. Furthermore, visualization of the changes in the SL and CT interval with temporal resolution down to 12.7 ms was possible with minimal degradation in image quality during the RUD and the clenched fist maneuvers. For the clenched fist maneuver, however, there was no difference in reader scores at the different temporal resolutions ($p > 0.05$) (Table 3). RT-MRI scans at any temporal resolution were deemed suboptimal for assessing the contrast between intraarticular fluid and surrounding structures, including the TFCC.

Slice thickness of 6 mm for RT-MRI corresponded to improved reader scores compared to 8 mm

Reader assessments showed significantly improved scores for images with a slice thickness of 6 mm (3.00 (1.00)) compared to those with 8 mm (2.00 (0.25)), $p < 0.05$. This was in spite of a higher signal-to-noise ratio exhibited by the latter than the former. The higher reader scores for the 6-mm-slice thickness images were attributed to the improved visualization of wrist structures due to lesser in-plane averaging.

Static MRI enabled visualization of wrist structures of interest

The wrist bones were visualized clearly in the T_1w gradient-recalled-echo acquisitions with an average reader score of 4.0 (overall), 2.9 (SL interval), and 2.9 (CT interval). This acquisition, however, did not provide adequate visualization of the anatomy of the TFCC or ligaments. On the other hand, the

Figure 2. Static imaging of the wrist at 0.55T in the coronal plane; (a) proton-density weighted 2D fat-suppressed, TSE image showing the visualization of the SL ligament (orange arrow) and the TFCC (green arrow); (b) T_1w 2D TSE image demonstrating the anatomical structures of the wrist; and (c) 3D T_1w gradient recalled echo pulse sequence with Dixon-based water reconstruction, illustrating the anatomical template to segment the bones.

PDw TSE acquisition demonstrated TFCC anatomy (including the potential to identify a laminar tear) and the SL ligament. All scans were rated good to very good and diagnostic.

DISCUSSION

The results of this first evaluation of a high-performance 0.55T MRI system for wrist imaging show that RT acquisition during continuous, active, and uninterrupted wrist motion is feasible at a high temporal resolution (<100 ms per image, down to 12.7 ms per image). The resulting images, alongside static wrist MRI scans, present anatomical information relevant to assessing dynamic wrist dysfunction. The availability of this technique could provide means to address critical questions pertinent to wrist kinematics and dysfunction. For example, several theories have been proposed to summarize complex wrist kinematics, such as the column, row, intercalated segment, and oval ring concepts. Evidence could be generated regarding these theories via *in vivo*, non-invasive studies using the proposed method thus improve the accuracy of biomechanical analysis, as opposed to cadaver studies. Furthermore, the proposed method could improve our understanding of the kinematics alterations underlying dynamic carpal instability *in vivo* and provide a tool for tracking outcomes of treatments.

High-performance 0.55T systems could provide other advantages for wrist imaging over high-field MRI. These include the ability to image immediately adjacent to metallic implants, improved safety profile in patients with implantable devices, such as

Figure 3. Wrist RT-MRI at 0.55T during the performance of the RUD maneuver with varying temporal resolution, with a spiral bSSFP sequence. Snapshots of the wrist in the neutral position with full sampling (164.6 ms per image), and with acceleration by factors of 92%, 85 and 77%. Temporal blurring is induced by lower temporal resolution and obscures the visualization of the wrist joints (red arrow shows the SL interval). Slice thickness is 6 mm.

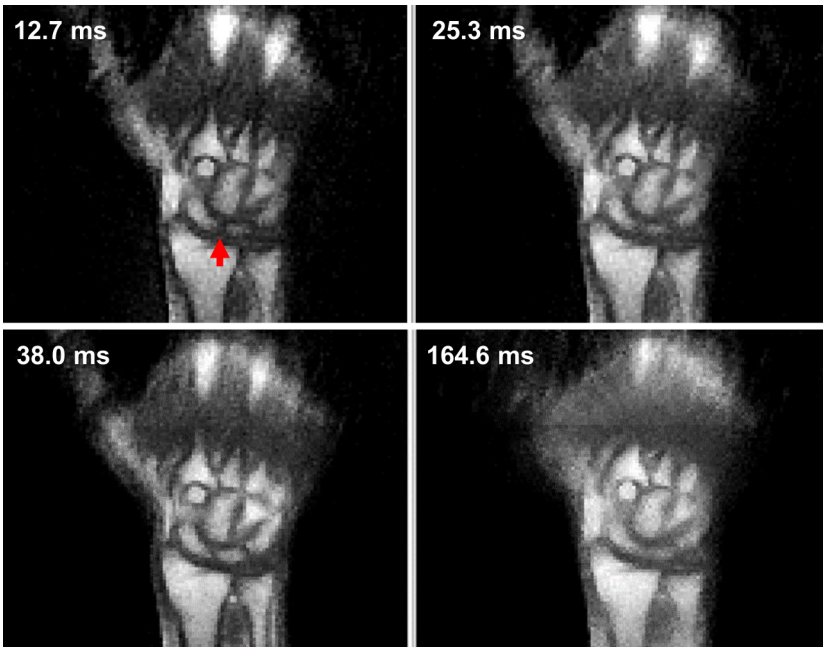

Table 3. Reader scores (median (interquartile range)) for RT-MRI scans during the performance of the RUD and the clenched-fist maneuver at the different temporal resolutions

Temporal resolution (ms)	Overall score	SL interval	CT interval
Radial-ulnar deviation			
12.7	3.50 (1.00)	3.00 (1.00)	2.50 (1.00)
25.3	3.50 (1.00)	3.00 (1.00)	2.50 (1.00)
38.0	3.50 (1.00)	3.00 (1.00)	2.50 (1.00)
63.3	3.50 (1.00)	2.50 (1.00)	2.50 (1.00)
101.3	2.50 (1.00)	2.00 (0.00)	2.00 (0.25)
164.6	2.00 (0.25)	1.00 (0.00)	1.50 (1.00)
Clenched fist			
12.7	3.00 (0.00)	2.50 (0.50)	2.50 (0.50)
25.3	2.50 (0.50)	2.00 (0.00)	2.50 (0.50)
38.0	2.50 (0.50)	2.00 (0.00)	2.50 (0.50)
63.3	2.50 (0.50)	2.00 (0.00)	2.00 (0.00)
101.3	2.50 (0.50)	2.00 (0.00)	2.00 (0.00)
164.6	2.00 (0.00)	2.00 (0.00)	2.00 (0.00)

pacemakers or defibrillators, substantially lower acoustic noise, easier system installation, and maintenance due to substantially reduced weight, footprint, and liquid helium requirement that result in lower operating costs.[8,10] Unlike Computed Tomography (CT), MRI does not involve ionizing radiation; therefore, there are clear advantages for repeat scanning (such as for frequent monitoring of response to treatment) or for imaging pediatric subjects and pregnant females.

We describe an evaluation of a static wrist MRI protocol with the high-performance 0.55T system. Given our promising results, we could consider a clinical scenario where static and RT-MRI could be performed in the same session, thus providing a comprehensive evaluation of wrist dysfunction. Cineradiography or dynamic CT have been proposed for assessing wrist instability[12,13] as additional tests beyond MRI; however, these methods are currently not part of the standard clinical assessment and require a separate exam that involves ionizing radiation.

Our study had limitations. First, it was a proof-of-concept study in a small number of asymptomatic participants with no known wrist pathology. Future studies are needed in more subjects with and without wrist pathology to substantiate our findings and to develop rigorous image scoring or grading systems. Second, study participants were instructed to move their wrists in an unassisted manner. The wrist was unconstrained with the aim of having more natural wrist motion. As a result, comparison between participants, who may have different ranges of motion or mechanics, could be difficult. We may have to adapt methods developed previously to address this problem.[14] Lastly, high-performance 0.55T technology is in its nascent stage. Efforts to develop novel acquisition and image reconstruction for the high-performance 0.55T platform are underway,[15] and these efforts could directly benefit wrist imaging.

CONCLUSION

We demonstrated the feasibility of a high-performance 0.55T MRI system for imaging tissues of the moving wrist in real time. These early results suggest that high-performance 0.55T MRI could be a promising technology to evaluate further for improving the assessment of wrist biomechanics and dynamic dysfunction.

COMPETING INTERESTS

Sophia X. Cui is an employee of Siemens Healthineers. The remaining authors declare no potential conflicts of interest with respect to the research, authorship, and/or publication of this article.

FUNDING

This study was supported by the National Science Foundation (NSF) Grant No. #MRI-1828736 and Siemens Healthineers.

REFERENCES

1. Garcia-Elias M. Understanding wrist mechanics: a long and winding road. *J Wrist Surg* 2013; **2**: 5–12. https://doi.org/10.1055/s-0032-1333429
2. Rainbow MJ, Wolff AL, Crisco JJ, Wolfe SW. Functional kinematics of the wrist. *J Hand Surg Eur Vol* 2016; **41**: 7–21. https://doi.org/10.1177/1753193415616939
3. Borotikar B, Lempereur M, Lelievre M, Burdin V, Ben Salem D, Brochard S. Dynamic MRI to quantify musculoskeletal motion: a systematic review of concurrent

validity and reliability, and perspectives for evaluation of musculoskeletal disorders. *PLoS One* 2017; **12**: e0189587. https://doi.org/10.1371/journal.pone.0189587
4. Boutin RD, Buonocore MH, Immerman I, Ashwell Z, Sonico GJ, Szabo RM, et al. Real-time magnetic resonance imaging (MRI) during active wrist motion--initial observations. *PLoS One* 2013; **8**: e84004. https://doi.org/10.1371/journal.pone.0084004
5. Quick HH, Ladd ME, Hoevel M, Bosk S, Debatin JF, Laub G, et al. Real-time MRI of joint movement with trueFISP. *J Magn Reson Imaging* 2002; **15**: 710–15. https://doi.org/10.1002/jmri.10120
6. Shaw CB, Foster BH, Borgese M, Boutin RD, Bateni C, Boonsri P, et al. Real-time three-dimensional MRI for the assessment of dynamic carpal instability. *PLoS One* 2019; **14**: e0222704. https://doi.org/10.1371/journal.pone.0222704
7. Zarenia M, Arpinar VE, Nencka AS, Muftuler LT, Koch KM. Dynamic tracking of scaphoid, lunate, and capitate carpal bones using four-dimensional MRI. *PLoS One* 2022; **17**: e0269336. https://doi.org/10.1371/journal.pone.0269336
8. Campbell-Washburn AE, Ramasawmy R, Restivo MC, Bhattacharya I, Basar B, Herzka DA, et al. Opportunities in Interventional and diagnostic imaging by using high-performance low-field-strength MRI. *Radiology* 2019; **293**: 384–93. https://doi.org/10.1148/radiol.2019190452
9. Restivo MC, Ramasawmy R, Bandettini WP, Herzka DA, Campbell-Washburn AE. Efficient spiral in-out and EPI balanced steady-state free precession cine imaging using a high-performance 0.55t MRI. *Magn Reson Med* 2020; **84**: 2364–75. https://doi.org/10.1002/mrm.28278
10. Nayak KS, Lim Y, Campbell-Washburn AE, Steeden J. Real-time magnetic resonance imaging. *J Magn Reson Imaging* 2022; **55**: 81–99. https://doi.org/10.1002/jmri.27411
11. Schmitt R, Froehner S, Coblenz G, Christopoulos G. Carpal instability. *Eur Radiol* 2006; **16**: 2161–78. https://doi.org/10.1007/s00330-006-0161-1
12. Sulkers GSI, Strackee SD, Schep NWL, Maas M. Wrist cineradiography: a protocol for diagnosing carpal instability. *J Hand Surg Eur Vol* 2018; **43**: 174–78. https://doi.org/10.1177/1753193417694820
13. Halpenny D, Courtney K, Torreggiani WC. Dynamic four-dimensional 320 section CT and carpal bone injury - a description of a novel technique to diagnose scapholunate instability. *Clin Radiol* 2012; **67**: 185–87. https://doi.org/10.1016/j.crad.2011.10.002
14. Foster BH, Shaw CB, Boutin RD, Joshi AA, Bayne CO, Szabo RM, et al. A principal component analysis-based framework for statistical modeling of bone displacement during wrist maneuvers. *J Biomech* 2019; **85**: 173–81. https://doi.org/10.1016/j.jbiomech.2019.01.030
15. Khodarahmi I, Keerthivasan MB, Brinkmann IM, Grodzki D, Fritz J. Modern low-field MRI of the musculoskeletal system: practice considerations, opportunities, and challenges. *Invest Radiol* 2023; **58**: 76–87. https://doi.org/10.1097/RLI.0000000000000912